

TIMESCALE INVARIANCE OF RAPID X-RAY VARIABILITY OF THE BLACK HOLE CANDIDATE GRO J1719–24

F. VAN DER HOOFT,¹ C. KOUVELIOTOU,^{2,3} J. VAN PARADIJS,^{1,4} B. C. RUBIN,^{2,3} D. J. CRARY,^{3,5} M. H. FINGER,^{2,3} B. A. HARMON,³
 M. VAN DER KLIS,¹ W. H. G. LEWIN,⁶ J. P. NORRIS,⁷ AND G. J. FISHMAN³

Received 1995 September 27; accepted 1995 December 14

ABSTRACT

We present the results of an analysis of the time variability of the soft X-ray transient GRO J1719–24 (Nova Oph 1993), as observed with BATSE. Our analysis covers the entire ~ 80 day outburst, beginning with the first detection of this black hole candidate on 1993 September 25. We obtained power density spectra (PDSs) of the data in the 20–100 keV energy band, covering the frequency interval 0.002–0.488 Hz. The PDSs show a significant quasi-periodic oscillation peak, the centroid frequency of which increased from ~ 0.04 Hz at the onset of the outburst to ~ 0.3 Hz at the end. Additional noise is present in the PDSs, which we describe in terms of two components. We find that the evolution of the PDSs can be described as a gradual stretching by a factor of ~ 7.5 in frequency of the power spectrum, accompanied by a decrease of the power level by the same factor, such that the integrated power in a scaled frequency interval remains constant.

Subject headings: accretion, accretion disks — binaries: close — stars: individual (GRO J1719–24) — X-rays: stars

1. OBSERVATIONS

GRO J1719–24 (=GRS 1716–249, Nova Oph 1993) was detected independently with BATSE, on board the *Compton Gamma Ray Observatory*, and the SIGMA telescope, on *Granat*, on 1993 September 25 (Ballet et al. 1993; Harmon et al. 1993c). The source reached a maximum flux of ~ 1.4 crab (20–100 keV) on September 30 and was remarkable for the stability of its emission on a timescale of days. A linear fit to the X-ray light curve between October 1 and November 22 showed that the flux decreased by only $\sim 0.3\% \pm 0.05\%$ per day (Harmon et al. 1993b). From December 9 (day 75 of the outburst), the 20–100 keV flux of GRO J1719–24 suddenly decreased within 6 days from 1.1 ± 0.1 to 0.4 ± 0.08 crab, and on December 16–18 it dropped below the BATSE 3σ 1 day detection limit of 0.1 crab (Harmon & Paciesas 1993). A daily average flux history in the 20–100 keV energy band, as determined using the Earth occultation technique (Harmon et al. 1993a), is displayed in Figure 1.

The 20–100 keV energy spectrum softened steadily during the entire outburst; the photon index increased from 2.0 to 2.3 ± 0.05 during the rise to peak intensity, and from there on the spectrum softened more gradually. No marked changes in the spectral shape were observed during the sudden decrease in X-ray flux in 1993 December. After this outburst, GRO J1719–24 remained undetectable for BATSE until 1994 September, when it was detected with both SIGMA (Churazov et al. 1994) and BATSE (Harmon et al. 1994). This later period of activity is not discussed here.

2. TIME-SERIES ANALYSIS

We have used 1.024 s time resolution count-rate data from the large-area detectors (four broad energy channels) and applied an empirical model (Rubin et al. 1996) to subtract the signal due to the X-ray/gamma-ray background. This model describes the background by a harmonic expansion in orbital phase (with parameters determined from the observed background variations) and includes the risings and settings of the brightest X-ray sources in the sky. It uses eight orbital harmonic terms, and its parameters were updated every 3 hr.

For our analysis, we considered uninterrupted data segments of 512 successive time bins (of 1.024 s each) on which we performed fast Fourier transforms (FFTs) covering the frequency interval 0.002–0.488 Hz. Per day, we typically obtained 35 such segments while the source was above the Earth horizon. For each data segment and for each of the eight detectors separately, we calculated and coherently summed the FFTs of the lowest two energy channels (20–50, 50–100 keV). For those detectors that had the source within 60° of the normal, these FFTs were again coherently summed (weighted by the ratio of the source to the total count rates) and converted to power density spectra (PDSs). The PDSs were normalized such that the power density is given in units of $(\text{rms}/\text{mean})^2 \text{ Hz}^{-1}$ (see, e.g., van der Klis 1995a) and finally averaged over an entire day.

The PDSs show a significant peak, indicative of quasi-periodic oscillations (QPOs) in the time series. The centroid frequency of this peak slowly shifts toward higher frequencies. This remarkable evolution is illustrated in the dynamical spectrum shown in Figure 2 (Plate L11). From this figure it can be seen that the centroid frequency of the QPOs doubled from ~ 0.04 to ~ 0.08 Hz during the rise to maximum flux and then gradually increased to ~ 0.3 Hz. During this period, significant deviations from the general, approximately linear trend of increasing centroid frequency occur, with a particularly large positive excursion near day 60 of the outburst. The QPOs are absent when the flux starts rapidly decaying at day 75. The observed rise of the PDSs below ~ 0.01 Hz (see also Fig. 3) is probably not caused by the source, since it also appears in the

¹ Astronomical Institute “Anton Pannekoek,” University of Amsterdam, and Center for High Energy Astrophysics, Kruislaan 403, NL-1098 SJ Amsterdam, The Netherlands.

² Universities Space Research Association, Huntsville, AL 35806.

³ NASA/Marshall Space Flight Center, Huntsville, AL 35812.

⁴ Department of Physics, University of Alabama in Huntsville, Huntsville, AL 35899.

⁵ NAS/NRC Research Associate; Marshall Space Flight Center, NASA Code ES84, Huntsville, AL 35812.

⁶ Massachusetts Institute of Technology, MS 37-627, Cambridge, MA 02139.

⁷ NASA/Goddard Space Flight Center, Greenbelt, MD 20771.

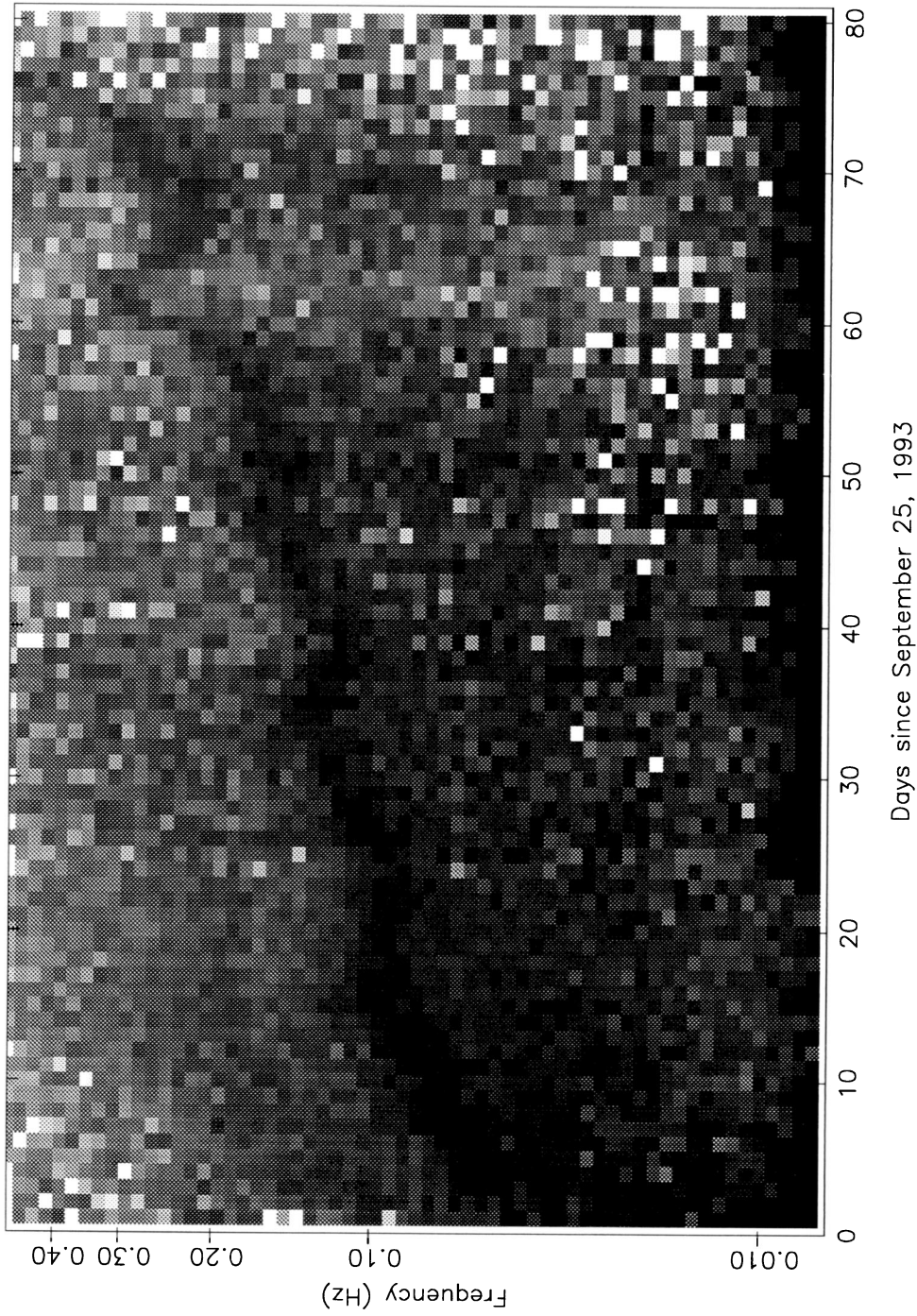


FIG. 2.—Dynamical spectrum of the set of daily averaged, $(\text{rms}/\text{mean})^2 \text{ Hz}^{-1}$ -normalized PDSs (20–100 keV) covering the outburst of GRO J1719–24. The frequency scale has been logarithmically rebinned; dark colors indicate a high power level. A dark band, the centroid frequency of which gradually shifts to higher frequencies, is clearly visible.

VAN DER HOOFT et al. (see 458, L75)

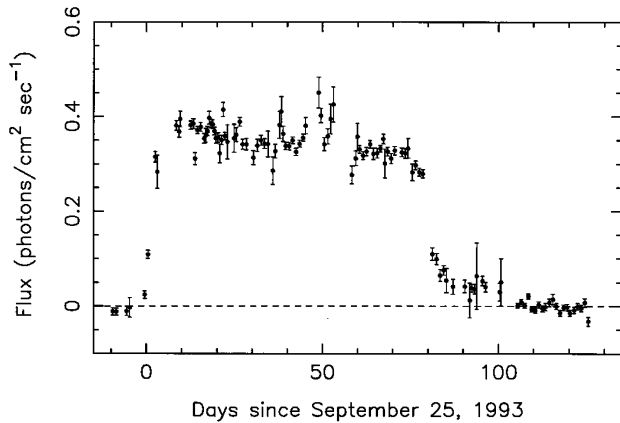


FIG. 1.—Flux history of GRO J1719–24 in the 20–100 keV energy band. The first detection of the source was made on 1993 September 25, and it reached a maximum flux of ~ 1.4 crab in 6 days. After 70 days at a slowly decreasing, high flux level, the source exhibited a rapid decrease of flux and became undetectable by BATSE after 83 days.

PDSs obtained while GRO J1719–24 was occulted by the Earth. Therefore, we excluded the frequency range below 0.01 Hz from the analysis.

A careful examination of the dynamical spectrum revealed the presence of structure in the PDSs, which we described in terms of two Lorentzians, one on each side of the QPO peak. The position of these additional structures seemed to scale with the frequency of the QPO. To further investigate this, we made fits to the PDSs using a combination of a power law and three Lorentzian profiles. To improve the statistics, we made fits to the average PDSs of 3 consecutive days, obtaining 23 3 day averaged PDSs. The model required 11 parameters (3 for

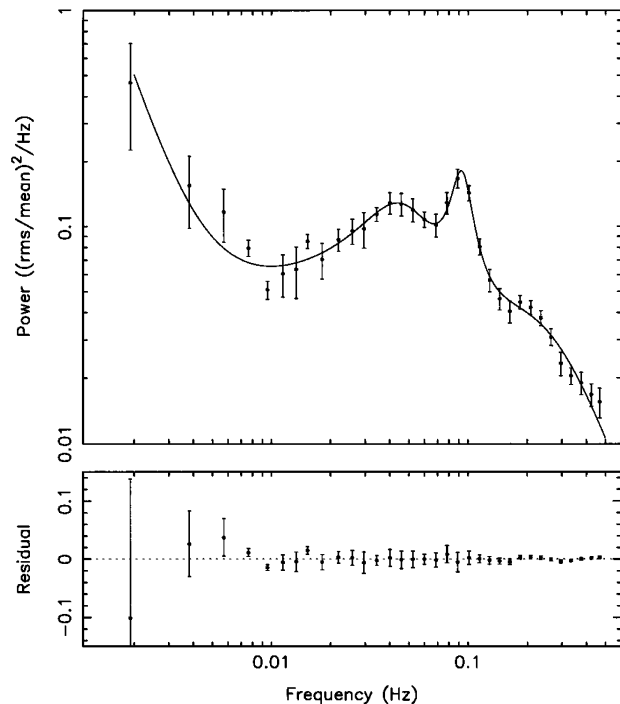


FIG. 3.—The 3 day averaged power spectrum for days 13–15 and the best-fit model (power law and three Lorentzian profiles) (*top*), and the residuals (*bottom*).

each Lorentzian, 2 for the power law) to be determined, which left 23 degrees of freedom (the PDSs were logarithmically rebinned to 34 frequency bins). Reduced χ^2 values of the fits were between 0.6 and 2.2. For the fit to the 3 day averaged PDSs starting at days 61 and 70, we used a combination of a power law and two Lorentzian profiles only since the noise component at the highest frequency is no longer well defined as it reaches the Nyquist frequency. A typical 3 day averaged power spectrum (days 13–15) and the model are shown in the top panel of Figure 3; the bottom panel displays the residuals. The centroid frequencies of the three Lorentzian profiles (ν_1 , ν_2 , and ν_3 , in order of increasing frequency) are strongly correlated (see Fig. 4).

Over a wide frequency interval, the centroid frequencies of the QPOs and the two noise components are consistent with being linearly related. We applied fits of the form $\nu_i = A + B\nu_j$ (taking the errors in both ν_i and ν_j into account; see, e.g., Press et al. 1992) to the data points, also shown in Figure 4. The parameters of these fits are tabulated in Table 1. A linear fit offers a good description of the data, resulting in reduced χ^2 values of 2.5 and 0.68 for the fits to (ν_1, ν_2) and (ν_2, ν_3) , respectively. When extrapolated, both fits pass through the origin, which indicates that the frequencies scale with a single factor. Therefore, we attempted a second series of fits, this time forced to pass through the origin by setting $A \equiv 0$. This also resulted in acceptable fits, shown as dashed lines in Figure 4, and a more precise determination of the slope. Based on this last series of fits, we find that there is no significant difference between the frequency ratios ν_1/ν_2 and ν_2/ν_3 ; we can exclude that these ratios have integer values.

This result led to the hypothesis that the PDSs may be described with a single characteristic profile, the frequency scale of which stretched proportionally during the outburst of GRO J1719–24. To test this hypothesis, we scaled each power spectrum in frequency by a factor such that the centroid frequency ν_2 of the QPO peak became equal to 0.1 Hz. Two such frequency-scaled PDSs are shown in Figure 5. It is evident that their shapes are very similar. The relative stretch factor of these two spectra is as large as 3.2.

As can be seen in Figure 5, the power spectrum obtained during the later stage of the outburst of GRO J1719–24 (when the QPOs were at the highest frequencies) has the lowest power densities. This led to the idea that the total power [and, therefore, in our chosen $(\text{rms}/\text{mean})^2 \text{ Hz}^{-1}$ normalization, the fractional rms amplitude], integrated over corresponding (but relatively scaled) frequency intervals, was constant throughout the outburst. Therefore, we determined the fractional rms amplitude from each 3 day averaged power spectrum in a frequency range corresponding to 0.01–0.15 Hz in the frequency-scaled domain. These fractional rms amplitudes are shown in Figure 6. Indeed, these values are approximately constant throughout the outburst. This makes it likely that the X-ray variability of GRO J1719–24 can be described by a single process, the characteristic timescale of which becomes shorter, but the fractional amplitude of which is invariant, during the entire outburst.

3. DISCUSSION

Soon after the X-ray detection of GRO J1719–24, a possible optical counterpart was discovered (Della Valle, Mirabel, & Rodríguez 1994), the photometric and spectroscopic properties of which suggest that GRO J1719–24 is a

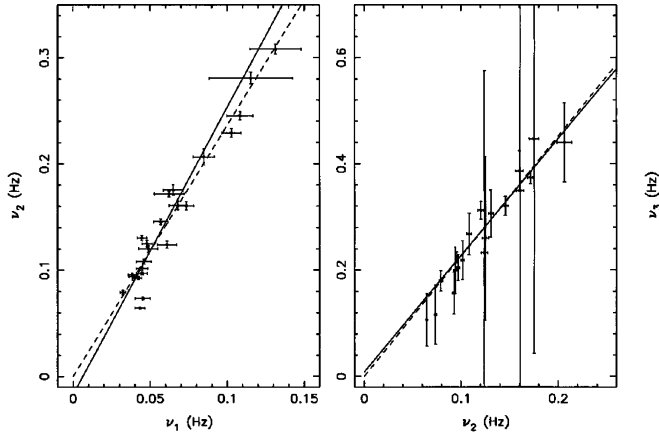


FIG. 4.—Values of the centroid frequencies of the three Lorentzian profiles, plotted vs. each other. The left panel contains (ν_1, ν_2) and covers days 4–72; the right panel contains (ν_2, ν_3) and covers days 4–60. Fits of the form $\nu_i = A + B\nu_j$ are also shown; parameters are listed in Table 1. The dashed lines represent the fit that is forced to pass through the origin.

low-mass X-ray binary. Since the orbital period and mass function of the system are not yet determined, GRO J1719–24 is still regarded as a black hole candidate (BHC) based on its hard energy spectrum only.

In Z sources, which form a subclass of the accreting neutron stars with low magnetic fields, two types of QPOs have been observed that have properties thought to be related to the accretion rate \dot{M} (see van der Klis 1995b and references therein). In horizontal-branch oscillations, the frequency (13–55 Hz) of the QPOs increases with source intensity. Such observations led to the introduction of the beat-frequency model. The flaring- and normal-branch oscillations have an approximately constant frequency between 5 and 7 Hz and have been modeled in terms of near-Eddington accretion. On phenomenological grounds, it does not seem likely that these mechanisms can explain the observed QPOs in GRO J1719–24; the timescale of the variations in GRO J1719–24 is much longer than those associated with Z sources, the dynamic range in frequency (0.04–0.3 Hz) is considerably larger than in the Z sources, and the source intensity decreases by 20% when the QPO frequency increases by a factor of 7.5.

Low-frequency (0.04–0.8 Hz) QPOs have been observed in the BHCs Cyg X-1, LMC X-1, GX 339–4, and GRO J0422+32 (van der Klis 1995b). These QPOs were observed while the sources were in their so-called low state, with the exception of LMC X-1, where a 0.08 Hz QPO was found while an ultrasoft component dominated the energy spectrum, showing that the source was in the high state. The large variation in QPO frequency seen in this source gives support to the idea

TABLE 1
PARAMETERS OF FITS SHOWN IN FIGURE 4

Centroid Frequencies	A	B	N^a	χ^2_{red}
(ν_1, ν_2)	-0.017 ± 0.008	2.70 ± 0.16	23	2.5
(ν_1, ν_3)	-0.036 ± 0.042	6.13 ± 0.91	19	1.2
(ν_2, ν_3)	0.008 ± 0.022	2.19 ± 0.18	19	0.68
(ν_1, ν_2)	0.0	2.363 ± 0.041	23	2.6
(ν_1, ν_3)	0.0	5.40 ± 0.19	19	1.2
(ν_2, ν_3)	0.0	2.257 ± 0.048	19	0.64

^a Number of data points.

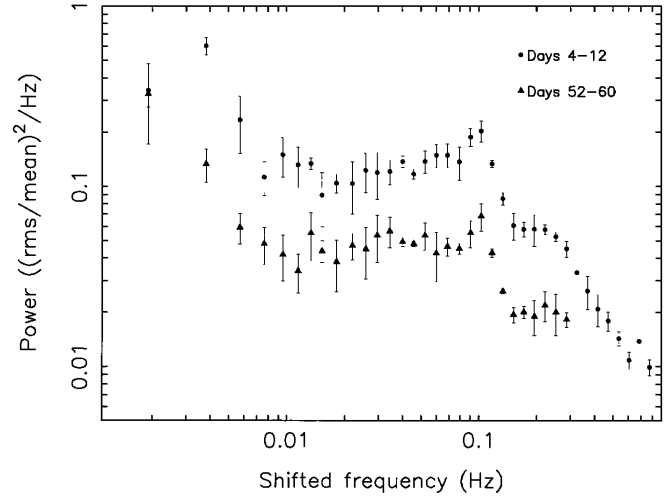


FIG. 5.—The 9 day averaged PDSs (starting at days 4 and 52, respectively), rescaled in frequency by such factors that the centroid frequency of the QPOs became equal to 0.1 Hz. The relative stretch factor of these two spectra is 3.2.

that all low-frequency (≈ 1 Hz) QPOs in BHCs have the same origin. It is important to mention that the intermediate-frequency QPOs in GX 339–4 (6 Hz, Miyamoto et al. 1991) and GS 1124–68 (3–10 Hz, Miyamoto et al. 1993) occurred while these sources were in the very high state.

In spite of the large range in frequency of the QPOs, the PDSs of GRO J1719–24 obey a remarkable regularity; their shape, after introducing a frequency scaling factor, does not appear to change much, and the power, integrated over a frequency range scaled by the appropriate frequency scaling factor, remains invariant. In the power density versus frequency plane, each point in the PDSs follows a ν^{-1} track toward higher frequencies and lower power densities during the outburst. This PDS behavior is consistent with a signal in the time domain whose timescale is stretched, but whose amplitude remains the same, like an accordian. This is reminiscent of the timescale invariance of the type II burst profiles of the Rapid Burster (Lewin et al. 1995), which harbors a neutron star (Hofmann, Marshall, & Lewin 1978). If these phenomena are related, this would imply that the mechanism responsible for the ≈ 1 Hz QPOs is not unique to BHCs.

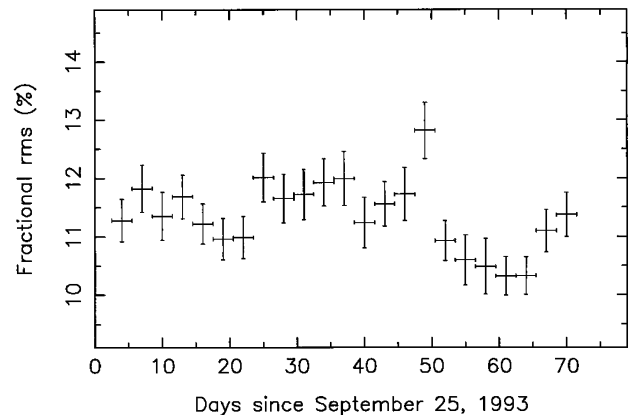


FIG. 6.—Fractional rms amplitudes, determined from the 3 day averaged PDSs, integrated over frequency ranges scaled by the appropriate frequency scaling factors. The fractional rms amplitude remains approximately constant at an average of $11.35\% \pm 0.60\%$.

Since the dynamical timescale in the inner region of a disk surrounding a stellar-mass black hole is in the millisecond range, the QPOs in GRO J1719–24 may have an origin farther out in the disk. The inner regions of viscous accretion disks surrounding black holes may suffer thermal-viscous instabilities when radiation pressure is important (Piran 1978). Chen & Taam (1994) have recently suggested that low-frequency QPOs (~ 0.04 Hz) in BHCs may be explicable by such thermal-viscous instabilities. A general property of this disk instability is that the frequency of the oscillation is a function of \dot{M} . Assuming a direct relation between source intensity and \dot{M} , one would expect that the frequency increases when the intensity decreases (Chen & Taam 1994). In GRO J1719–24, the QPO frequency increased by a factor of 7.5 while the 20–100 keV flux decreased by only 20%; it is not clear whether such a large change in QPO frequency for such a small change in \dot{M} can be explained by this thermal-viscous model. More recently,

Abramowicz, Chen, & Taam (1995) proposed a model in which the mass accretion and angular momentum transport take place in an optically thick disk but a fraction of the gravitational energy is dissipated in a corona. Stabilization of the disk depends not only on the rate of coronal energy dissipation but also on the location of the inner radius of the optically thick disk. Their results suggest that the QPO frequency can change, even if the mass accretion rate remains constant.

F. v. d. H. acknowledges support by the Netherlands Foundation for Research in Astronomy with financial aid from the Netherlands Organization for Scientific Research (NWO) under contract 782-376-011. F. v. d. H. also thanks the “Leids Kerkhoven–Bosscha Fonds” for a travel grant. J. v. P. acknowledges support from NASA grant NAG5-2560. W. H. G. L. was supported by NASA grant NAG8-216. This project was supported in part by the NWO under grant PGS 78-277.

REFERENCES

- Abramowicz, M. A., Chen, X., & Taam, R. E. 1995, *ApJ*, 452, 379
 Ballet, J., Denis, M., Gilfanov, M., & Sunyaev, R. 1993, *IAU Circ.*, No. 5874
 Chen, X., & Taam, R. E. 1994, *ApJ*, 431, 732
 Churazov, E., Gilfanov, M., Ballet, J., & Jourdain, E. 1994, *IAU Circ.*, No. 6083
 Della Valle, M., Mirabel, I. F., & Rodríguez, L. F. 1994, *A&A*, 290, 803
 Harmon, B. A., et al. 1993a, in *AIP Conf. Proc.* 280, *Compton Gamma-Ray Observatory*, ed. M. W. Friedlander, N. Gehrels, & D. J. Macomb (New York: AIP), 345
 Harmon, B. A., Fishman, G. J., Paciesas, W. S., & Zhang, S. N. 1993b, *IAU Circ.*, No. 5900
 Harmon, B. A., & Paciesas, W. S. 1993, *IAU Circ.*, No. 5913
 Harmon, B. A., Zhang, S. N., Paciesas, W. S., & Fishman, G. J. 1993c, *IAU Circ.*, No. 5874
 Harmon, B. A., Zhang, S. N., Paciesas, W. S., Wilson, C. A., & Fishman, G. J. 1994, *IAU Circ.*, No. 6104
 Hoffman, J. A., Marshall, H. L., & Lewin, W. H. G. 1978, *Nature*, 271, 630
 Lewin, W. H. G., van Paradijs, J., & Taam, R. E. 1995, in *X-Ray Binaries*, ed. W. H. G. Lewin, J. van Paradijs, & E. P. J. van den Heuvel (Cambridge: Cambridge Univ. Press), 175
 Miyamoto, S., Iga, S., Kitamoto, S., & Kamado, Y. 1993, *ApJ*, 403, L39
 Miyamoto, S., Kimura, K., Kitamoto, S., Dotani, T., & Ebisawa, K. 1991, *ApJ*, 383, 784
 Piran, T. 1978, *ApJ*, 221, 625
 Press, W. H., Teukolsky, S. A., Vetterling, W. T., & Flannery, B. P. 1992, *Numerical Recipes in FORTRAN* (2d ed.; Cambridge: Cambridge Univ. Press)
 Rubin, B. C., et al. 1996, in preparation
 van der Klis, M. 1995a, in *The Lives of the Neutron Stars*, ed. M. A. Alpar, Ü. Kiziloğlu, & J. van Paradijs (NATO ASI Ser. C, 450) (Dordrecht: Kluwer), 301
 ———. 1995b, in *X-Ray Binaries*, ed. W. H. G. Lewin, J. van Paradijs, & E. P. J. van den Heuvel (Cambridge: Cambridge Univ. Press), 252